33rd Annual International Conference of the IEEE EMBS
Boston, Massachusetts USA, August 30 - September 3, 2011

PCR-Free, Microfluidic Single Molecule Analysis of Circulating Nucleic Acids in Lung Cancer Patient Serum

Kelvin J. Liu[1] and Tza-Huei Wang[1,2,*]

Abstract—**Circulating nucleic acid (CNA) has been the focus of much recent research, studied both as a diagnostic marker and as a marker for enrichment of diseased DNA. Among these markers, circulating DNA fragment size has shown promise for discerning the source of CNA molecules in cancer and prenatal diagnostics due to differences in average size between cancer vs. healthy or fetal vs. maternal DNA. We describe a 1-step assay for analyzing circulating DNA size and quantity directly in human serum that replaces complicated nested qPCR analysis. Microfluidic cylindrical illumination confocal spectroscopy and fluorescence burst size analysis were used to individually count and size fluorescently-labeled CNA molecules as they were driven through a microfluidic constriction. First, single molecule sizing was performed on λ Hind III digest DNA to obtain a size calibration curve. A linear relation between DNA length and fluorescent burst size was seen from 564 bp – 23.1 kbp. Then, the single molecule assay was used to analyze an in vitro model of DNA fragmentation. Finally, DNA sizing analysis was successfully performed on serum samples from both early and late stage lung cancer patients. This assay was performed directly in patient serum using only a single reagent, a simple DNA intercalating dye. Furthermore, it eliminated the need for DNA isolation or enzymatic amplification. This demonstrates that microfluidic single molecule spectroscopy can be a rapid, facile, and inexpensive alternative to the established PCR-based methods.**

I. Introduction

Circulating and cell-free nucleic acid (CNA) consists of extra-cellular genetic material freely found in human body fluids such as blood, urine, and sputum. These information rich molecules are a near ideal source of non-invasive biomarkers. They are being extensively studied in a diverse array of human diseases [2]. In cancer, CNA can be used to non-invasively determine the status of remote tumors by decoding the contained genetic and epigenetic information, potentially eliminating the need for tissue biopsies. However, the clinical analysis of CNA biomarkers faces two key hurdles. First, analysis methods must be highly sensitive to detect low physiological CNA levels and, second, they must be highly specific to accurately discern target CNA from a sea of obscuring background CNA [3]. To date, PCR-based methods have been used near exclusively for analysis. While PCR is highly sensitive, it has limitations such as amplification errors, varying amplification efficiencies, and reproducibility [4]. Rapid and inexpensive alternatives to PCR can therefore provide scientists with additional tools to more efficiently validate these promising biomarkers.

Circulating DNA size has been explored in both cancer management [5] and fetal medicine [6]. The presence of long circulating DNA strands within blood, urine, and stool (i.e. increased DNA integrity) has been suggested to be indicative of neoplastic disease. Accordingly, DNA integrity has been used as a general cancer marker in a wide variety of cancers including gynecologic, head and neck, breast, and colon [5, 7-9]. In fetal medicine, circulating fetal DNA has been shown to be shorter than maternal DNA. This size difference has been used to enrich rare fetal DNA from a sea of maternal DNA for increased specificity in non-invasive prenatal diagnostics [6, 10]. Thus, DNA size can be used to identify the source of CNA molecules. Previous studies have used nested qPCR to size DNA, a cumbersome approach that may be contributing to the variability in reported results.

Herein, we describe the first PCR-free, single molecule assay for CNA analysis [1]. It was applied for the analysis of circulating DNA integrity in lung cancer patient serum samples. Microfluidic cylindrical illumination confocal spectroscopy (μCICS) was used to size and quantify CNA fragments in human serum via fluorescent burst size analysis as illustrated in Fig. 1. μCICS uses a 1-D laser sheet and matched microfluidic constriction to achieve high detection uniformity, 100% mass detection efficiency, and higher throughput than conventional, diffraction-limited confocal spectroscopy (CS)-systems [11]. This assay used only a single reagent, was performed directly in serum without the need for DNA isolation, and consumed <10 pL of sample.

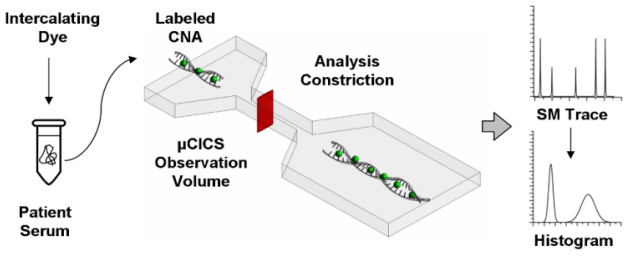

Fig. 1 Schematic illustration of the 1-step, PCR-free, single molecule CNA sizing assay [1].

II. Results

A. μCICS Platform

An optical schematic and image are shown in Figure 2. In standard CS, the diffraction-limited laser excitation spot precludes accurate DNA sizing. In μCICS, 1-D beam

[1]Biomedical Engineering Department
[2]Mechanical Engineering Department
*Corresponding author: thwang@jhu.edu

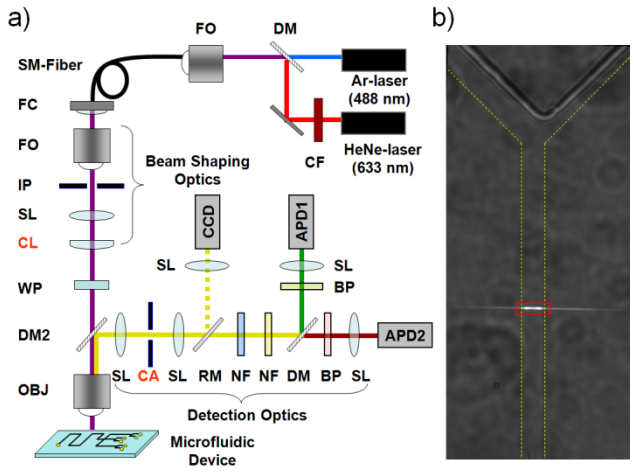

Fig. 2 a) Component diagram of µCICS platform. b) CCD image of the µCICS illumination sheet focused into the microfluidic analysis constriction [1].

expansion is used to stretch the laser spot into line that spans the entire width of the microchannel. A 5 x 0.5 µm (w x h) microfluidic constriction is then used to transport molecules through the center of this observation region (Fig 2b – yellow dotted lines). Because the observation region fully encloses the analysis constriction, 100% mass detection efficiency (i.e. detection all molecules flowing through the constriction) can be achieved and has been previously demonstrated for fluorescently labeled DNA as well as single fluorophores [11]. The 1-D observation volume expansion (i.e. from a point to a line) allowed uniform excitation and detection across the entire constriction cross-section such that fluorescent burst size was correlated only to DNA length and irrespective of molecular trajectory.

The µCICS platform has two overlapping excitation and detection channels. 488/520 nm excitation/detection was used to monitor the tracer particle fluorescence while 633/670 nm excitation/detection was used to analyze the DNA fluorescence. Briefly, a 633 nm He-Ne laser and 488 nm Ar-ion laser were combined using a dichroic mirror, DM, and coupled into a polarization preserving single mode optical fiber, SM-Fiber. The output from the fiber was collimated, expanded, and then focused in 1-D with a cylindrical lens, CL. A ½ waveplate, WP, was used to align the laser polarization at a 57° angle with respect to the microchannel [12]. The laser excitation sheet was focused into the center of the analysis constriction on the microfluidic device with a 100 x, 1.3 NA oil immersion microscope objective, OBJ. The focused illumination volume, shown in Figure 2b, had $1/e^2$ radii of x_0=18, y_0=0.5, and z_0=2.1 µm where x_0, y_0, and z_0 align with the channel width, length, and height, respectively. The emitted fluorescence was then collected by the same objective, separated from the excitation light using a dichroic mirror, DM2, and filtered by a 600 x 150 µm (w x h) rectangular confocal aperture, CA. The confocal aperture limited light collection to the centermost 7 µm of the 36 µm wide illumination sheet where the illumination intensity was most uniform (red rectangle in Fig. 2b). This created a 7 x 2 µm (w x h) observation region that was slightly larger than the 5

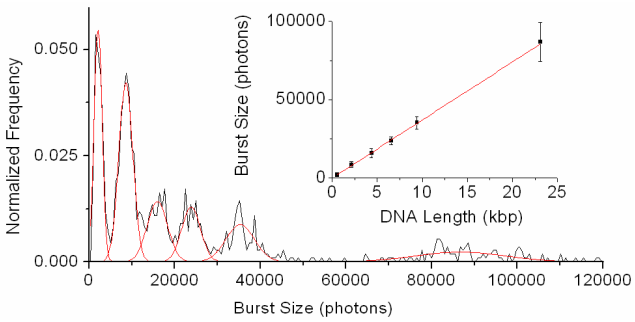

Fig. 3 Fluorescent burst size analysis of λ Hind III digest DNA performed using µCICS. inset) The average burst size of each peak shows the expected linear correlation to DNA size (R^2 = 0.999). Error bars represent the peak SDs.

x 0.5 µm (w x h) analysis constriction (dashed yellow lines in Fig. 2b) to ensure 100% mass detection efficiency, simple alignment, and high detection uniformity. Holographic notch filters, NF, were used to reduce the laser scattering background. A series of dichroic mirrors, DM, and bandpass filters, BP, was then used to separate and select the desired fluorescence wavelengths before being detected with two APDs. The output signal from the APDs was sent into a computer for analysis using software written in Labview. A CCD camera was used to align the µCICS observation volume with the analysis constriction.

B. Single Molecule Fluorescent Burst Size Analysis

Fluorescent burst size analysis was performed on λ Hind III digest DNA to obtain a size calibration curve. As depicted in Fig. 1, the DNA was stoichiometrically labeled with TOTO-3 intercalating dye such that each DNA molecule incorporated a number of dye molecules that was directly proportionate to its length. Because the sample flow rate and stability have such a large impact on sizing performance, green fluorescent tracer particles were used to monitor the in situ flow velocity while DNA sizing was performed in the red channel. The labeled sample was diluted, fluorescent tracer particles were added, and the sample was loaded into a PDMS microfluidic device fabricated using soft-lithography. The µCICS observation volume was then focused into the center of the analysis constriction. As each DNA molecule traversed the observation volume, it was excited and emitted a burst of photons. This procession of fluorescent signals formed a single molecule trace. A thresholding algorithm was used to identify fluorescent bursts within the trace. These bursts were then analyzed for parameters such as burst size, burst width, and transit time.

Fig. 3 shows a typical burst size histogram. Each histogram peak is a collection of fluorescent bursts that corresponds to a sub-population of DNA within the λ Hind III digest. When the peaks were curve-fit with a series of Gaussian functions (red curves), a strong linear correlation was seen between average burst size (i.e. peak center position) and DNA length, demonstrating the ability to accurately size DNA from 564 bp-23.1 kbp. The 2 kbp fragments were easily detected with a typical S/N ratio of

~80 and measurement coefficient of variation (CV) of ~25 %. The measurement CV prevented the 2027 bp and 2322 bp peaks from being individually resolved and the 125 bp peak from being resolved from background. The measurement CV decreased with increasing DNA length due to factors such as Poisson variability in the photo-emission and -detection processes and staining variability. The 23 kbp peak typically displayed a much lower CV of 5-10 %.

While burst size can be used to determine DNA length, burst rate can be used to determine abundance. We have previously shown that CS can be used to quantify sub-femtomolar levels of DNA [13]. Given the flow velocity, channel dimensions, and DNA concentration, ~520 molecules would be expected during each 300 s measurement whereas 590 molecules were actually detected, demonstrating 100% mass detection efficiency. The overestimation can be accounted for by small errors in the channel dimensions, measured flow velocity, observation volume size, and sample preparation. In addition, each population was properly enumerated at equal molar fractions with the composite 2.1 kbp peak having double the abundance (~30 %) of the other peaks (~15 %).

C. DNA Fragmentation Model

The ability of μCICS to characterize DNA integrity was then tested using an in vitro model of DNA fragmentation [14]. λ DNA (Invitrogen) was sheared into random length fragments by exposure to ultrasonic agitation (Branson) for 0, 15, 60, 120, or 600 seconds. The DNA fragments were then labeled using TOTO-3 and analyzed on the μCICS platform at a total DNA concentration of 0.2 ng/mL. As the ultrasonic agitation time increased, the DNA became increasingly fragmented (i.e. decreased DNA integrity) and variable in length. Fig. 4 shows 5 burst size histograms of the ultrasonically sheared DNA. The control DNA (0 min) appears as a sharp Gaussian shaped peak due to the uniform size distribution of the λ DNA. As the ultrasonic shearing time increases, the sharp peak representing intact λ DNA decreases in size and broadens in width while the broad distribution representing small background bursts increases in size. At 600 seconds, the DNA is entirely sheared and no large DNA pieces remained.

This can be quantitatively seen by examining the burst size as function of ultrasonic agitation time. The average burst size progressively decreases while the CV increases with increasing agitation time, representing both decrease in average fragment size and an increased variability in the distribution of fragment sizes. By 600s the CV decreases again because the large DNA is entirely fragmented and there is no longer a mixed population of small and large DNA. It can also be seen that detected number of DNA fragments increases proportionately to the decrease in average fragment size as expected. The disparity between average burst size of total DNA versus the λ peak alone is due to the presence of small DNA fragments that are present in even the 0 s sample. This is due to sample impurity or

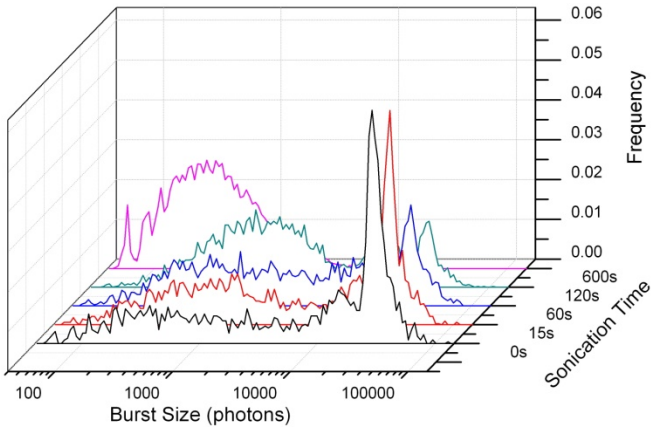

Fig. 4 Fluorescent burst size analysis of λDNA fragmented using ultrasonic agitation. The sharp peak at 30k photons representing whole λ DNA gives way to increasing proportions of small DNA fragments as sonication time is increased.

degradation which we have found to differ between sample vendors. Only 1 pg of DNA was analyzed in each BSDA histogram. In contrast, these differences cannot be easily seen or quantified using gel electrophoresis which requires 1000x more DNA for analysis.

D. Lung Cancer Serum Analysis

Based on the previous results which demonstrate that μCICS can be used to analyze DNA fragmentation, we postulated that direct detection of DNA integrity could be performed using patient serum. The elimination of enzymatic amplification and DNA isolation removes two potentially serious sources of experimental bias and greatly simplifies the assay, facilitating clinical translation and reducing cost. As a proof of feasibility, we performed a pilot study on a small cohort of lung cancer patient serum samples. TOTO-3 was used because it fluoresces in the deep red (660 nm), far from most cellular autofluorescence. Furthermore, its high specificity and high fluorescent enhancement enabled separation-free analysis. TOTO-3 is also cell membrane impermeant, ensuring that only cell-free nucleic acids were labeled.

A 1-step assay for analyzing CNA size was developed. Serum samples were mixed with TOTO-3 and incubated for 1 hour. The labeled samples were then diluted, mixed with fluorescent tracer particles, and loaded into a microfluidic device. Fig. 5a shows DNA sizing histograms for stage I and stage IV lung cancer patients. Qualitatively, it can be seen that the stage IV sample has a greater proportion of larger CNA fragments. Below 320 bp, the two curves appear similar. However, from 320-1000 bp, the stage IV sample consistently contains more fragments (Fig. 5a inset). Few background bursts were seen from sample autofluorescence or non-specific adsorption of TOTO-3

Because nested qPCR is typically used, DNA integrity (DI), a quantitative marker of DNA fragmentation, is usually calculated as the ratio of long DNA fragments to short DNA fragments within the same gene or amplification locus (e.g. abundance of 400 bp vs. 200 bp fragment of the β-actin

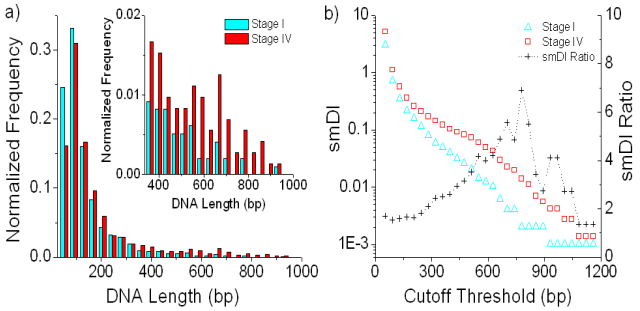

Fig. 5 a) DNA sizing histograms of serum samples taken from a stage I and a stage IV lung cancer patient. a, inset) Close-up view of the 320-1000 bp region. b) single molecule DNA integrity (smDI) was calculated as a function of the cutoff threshold. The smDI ratio (stage IV smDI / stage I smDI) was the greatest when a cutoff of ~800 bp was applied.

gene) [5, 7-9]. Nested qPCR can only concurrently probe a limited number of DNA loci and sizes. The limited number of sampled loci may not be representative of the larger circulating population as a whole and lead to high variability while the limited DNA sizing resolution may hinder the accuracy of the DI marker. This can be particularly true in PCR reactions where only a few genome equivalents of DNA are tested.

On the other hand, since the single molecule assay was not limited to specific fragment sizes, we defined single molecule DNA integrity (smDI) as the cumulative number of long DNA bursts / short DNA bursts where the distinction between long and short is defined by a cutoff threshold. µCICS can directly reveal the entire spectrum of CNA fragments, without sampling bias or ensemble averaging, eliminating potentially significant sources of error. Direct digital counting eliminates the need for tedious calibration curves. Accordingly, Fig. 5b shows smDI values for the previous patients as a function of cutoff threshold. The greatest distinguishing power occurred at ~800 bp where the stage IV patient had an smDI value nearly 7-fold that of the stage I patient. The applied threshold can have a significant impact on the sensitivity and specificity of the marker and should be empirically set using a large sample size. While these results are too preliminary to draw any clinical conclusions from, they demonstrate that µCICS can be used as a facile alternative to PCR for quantifying CNA markers such DNA integrity. A larger study will be necessary to determine the clinical sensitivity and specificity of the smDI marker in characterizing cancer progression.

III. Conclusion

We have detailed the development of a rapid and facile assay for CNA analysis based on µCICS, a microfluidic single molecule spectroscopy technique. We initially surmised that the overlap in dynamic range between single molecule sensing and physiological CNA levels would enable direct analysis of CNA markers without PCR amplification. As shown, with proper assay design and probe selection, single molecules can be detected even in complex biological backgrounds without amplification. DNA integrity was chosen as an example of a promising marker where the lack of alternatives to PCR-based methods may be limiting its application. However, PCR and single molecule methods need not be mutually exclusive. It is hoped that single molecule methods can be used to speed the clinical translation and adoption of new CNA biomarkers.

References

[1] K. J. Liu, M. V. Brock, M. Shih Ie, and T. H. Wang, "Decoding circulating nucleic acids in human serum using microfluidic single molecule spectroscopy," *J Am Chem Soc,* vol. 132, pp. 5793-8, Apr 28 2010.

[2] V. Swarup and M. R. Rajeswari, "Circulating (cell-free) nucleic acids--a promising, non-invasive tool for early detection of several human diseases," *FEBS Lett,* vol. 581, pp. 795-9, Mar 6 2007.

[3] M. Fleischhacker and B. Schmidt, "Circulating nucleic acids (CNAs) and cancer--a survey," *Biochim Biophys Acta,* vol. 1775, pp. 181-232, Jan 2007.

[4] F. Diehl and L. A. Diaz, Jr., "Digital quantification of mutant DNA in cancer patients," *Curr Opin Oncol,* vol. 19, pp. 36-42, Jan 2007.

[5] B. G. Wang, H. Y. Huang, Y. C. Chen, R. E. Bristow, K. Kassauei, C. C. Cheng, et al., "Increased plasma DNA integrity in cancer patients," *Cancer Res,* vol. 63, pp. 3966-8, Jul 15 2003.

[6] F. M. Lun, N. B. Tsui, K. C. Chan, T. Y. Leung, T. K. Lau, P. Charoenkwan, et al., "Noninvasive prenatal diagnosis of monogenic diseases by digital size selection and relative mutation dosage on DNA in maternal plasma," *Proc Natl Acad Sci U S A,* vol. 105, pp. 19920-5, Dec 16 2008.

[7] K. C. Chan, S. F. Leung, S. W. Yeung, A. T. Chan, and Y. M. Lo, "Persistent aberrations in circulating DNA integrity after radiotherapy are associated with poor prognosis in nasopharyngeal carcinoma patients," *Clin Cancer Res,* vol. 14, pp. 4141-5, Jul 1 2008.

[8] N. Umetani, A. E. Giuliano, S. H. Hiramatsu, F. Amersi, T. Nakagawa, S. Martino, et al., "Prediction of breast tumor progression by integrity of free circulating DNA in serum," *J Clin Oncol,* vol. 24, pp. 4270-6, Sep 10 2006.

[9] N. Umetani, J. Kim, S. Hiramatsu, H. A. Reber, O. J. Hines, A. J. Bilchik, et al., "Increased integrity of free circulating DNA in sera of patients with colorectal or periampullary cancer: direct quantitative PCR for ALU repeats," *Clin Chem,* vol. 52, pp. 1062-9, Jun 2006.

[10] Y. Li, E. Di Naro, A. Vitucci, B. Zimmermann, W. Holzgreve, and S. Hahn, "Detection of paternally inherited fetal point mutations for beta-thalassemia using size-fractionated cell-free DNA in maternal plasma," *Jama,* vol. 293, pp. 843-9, Feb 16 2005.

[11] K. J. Liu and T. H. Wang, "Cylindrical illumination confocal spectroscopy: rectifying the limitations of confocal single molecule spectroscopy through one-dimensional beam shaping," *Biophys J,* vol. 95, pp. 2964-75, Sep 15 2008.

[12] J. H. Werner, E. J. Larson, P. M. Goodwin, W. P. Ambrose, and R. A. Keller, "Effects of fluorescence excitation geometry on the accuracy of DNA fragment sizing by flow cytometry," *Appl Opt,* vol. 39, pp. 2831-9, Jun 1 2000.

[13] C. Y. Zhang, H. C. Yeh, M. T. Kuroki, and T. H. Wang, "Single-quantum-dot-based DNA nanosensor," *Nat Mater,* vol. 4, pp. 826-31, Nov 2005.

[14] J. Ellinger, A. von Rucker, N. Wernert, R. Buttner, P. J. Bastian, and S. C. Muller, "[Prostate cancer research. Biomarkers as promising options for optimized diagnosis and treatment]," *Urologe A,* vol. 47, pp. 1190-2, Sep 2008.